Physica B 654 (2023) 414649

Contents lists available at ScienceDirect

Physica B: Condensed Matter

journal homepage: www.elsevier.com/locate/physb

Dielectric relaxation, optical and structural characterizations of complex composite films based on polyethylene oxide doped by low concentration of iodine

Ahmad Telfah [a,f,*], Qais M. Al-Bataineh [a,b,c], Belal Salameh [d], Ahmad A. Ahmad [b], Ahmad M. Alsaad [b], R.F. Sabirianov [e]

[a] Leibniz Institut für Analytische Wissenschaften-ISAS-e.V., Bunsen-Kirchhoff-Straße 11, 44139, Dortmund, Germany
[b] Department of Physical Sciences, Jordan University of Science & Technology, P.O. Box 3030, Irbid, 22110, Jordan
[c] Technische Universität Dortmund (TU Dortmund), Fakultät Physik, Otto-Hahn-Straße 4a, D-44227, Dortmund, Germany
[d] Physics Department, Kuwait University, P.O.Box 5969, 13060, Safa, Kuwait
[e] Department of Physics, University of Nebraska at Omaha, Omaha, NE, 68182, USA
[f] Nanotechnology Center, The University of Jordan, 11942, Amman, Jordan

ARTICLE INFO

Keywords:
Polyethylene oxide (PEO)
Iodine (I_2)
UV–Vis spectroscopy
Fourier transform infrared spectroscopy (FTIR)
Doping mechanism
Optical properties

ABSTRACT

The dielectric relaxation, optical, chemical and structural characterizations of synthesized complex composite films based on polyethylene oxide (PEO) doped with low concentrations of iodine (I_2) were investigated. XRD results show that all PEO films have a semi-crystalline nature. Increasing I_2 concentrations up to 1.0% into PEO films decreases the crystallinity degree from 40.0% to 21.1%. In addition, the bandgap energy decreases from 4.42 to 3.68 eV, as I_2 increases to 1.0%. The permittivity and conductivity relaxation processes are studied over the temperatures from 288 K up to 318 K using Havriliak–Negami relationship to investigate the relaxation times, dielectric strengths, and the electrical conductivities. The ionic concentrations dominate the relaxation time due to the favorable I^{-3}-polymer clustering. The findings investigate the impact of I_2 and its ions on the segmental dynamics of PEO chains and optical, optoelectronic, and dielectric properties of polymers complexation with the non-metallic element in native form.

1. Introduction

Recently, the synthesis and characterization of solid polymer electrolytes films (SPEs) have attracted great consideration from fundamental and industrial points of view. Particularly, for energy storage, water treatment, sensors, and actuators owing to their attractive properties such as large bandgaps, significant absorption coefficients, and high energy binding [1–3].

Polyethylene oxide (PEO) is considered to be a crucial polymer electrolyte because of its several convenient chemical and physical properties, such as low cost, good solubility for the metal ions, high chemical stability, electrochemical and reduction processes, and low absorption compared to other host polymers [4–7]. In addition, PEO has a semi-crystalline nature at room temperature [7,8]. PEO is essential for many practical applications such as fuel cells, lithium-ion batteries, hybrid power supercapacitors [9–11]. Many studies were investigated the effect of metal and semiconductors nanoparticles and complex ions on the optical, electrical, dielectric properties of the PEO. M. Farea et al. [12,13] stated that increasing cesium bromide and gold nanoparticles in PEO films leads to decrease the bandgap energy and increase the electrical conductivity. In addition, adding ion salts in PEO matrix leads to enhance the electrical conductivity, as reported in literature [14,15].

Previous works have focused on improving the optical properties and electrical conductivity of SPEs by doping with electron donor materials or electron acceptor materials [16]. Iodine was chosen as the dopant ion because of its significant influence on the dielectric and optical properties of SPEs. The incorporation of iodine into SPEs leads to the increase of polymer oxidation and a change in charge-storing capacity, consequently leading to an enhanced electrical conductivity [17,18]. Due to its suitable ionic conductivity, dielectric properties and optical properties, polyethylene oxide doped with iodine is a successful complex compound for many technical applications [19,20]. In addition, the

* Corresponding author. Leibniz Institut für Analytische Wissenschaften-ISAS-e.V., Bunsen-Kirchhoff-Straße 11, 44139, Dortmund, Germany.
E-mail address: telfah.ahmad@isas.de (A. Telfah).

https://doi.org/10.1016/j.physb.2023.414649
Received 27 September 2022; Received in revised form 21 December 2022; Accepted 4 January 2023
Available online 6 January 2023

Table 1
Preparation parameters of PEO/methanol, I_2/methanol, PEO/I_2/methanol composites.

Weight percent	PEO/methanol		I_2/methanol		Film thicknesses
[wt.%]	[mL]	[g]	[mL]	[g]	[nm]
0	20	0.2	0.00	0.0000	472.55
0.01	20	0.2	0.02	0.0002	503.34
0.03	20	0.2	0.06	0.0006	546.14
0.06	20	0.2	0.12	0.0012	512.39
0.1	20	0.2	0.20	0.0020	486.66
1	20	0.2	2.00	0.0200	431.16

Table 2
Preparation parameters of PEO/methanol, I_2/methanol, PEO/I_2/methanol composites.

Weight percent	PEO/methanol		I_2/methanol		Film thicknesses
[wt.%]	[μL]	[g]	[μL]	[g]	[μm]
0	500	0.1	0	0.00000	12.5
0.01	500	0.1	1	0.00001	11.6
0.03	500	0.1	3	0.00003	12.4
0.06	500	0.1	6	0.00006	10.8
0.1	500	0.1	10	0.00010	11.9
1	500	0.1	100	0.00100	10.3

iodine dopant ions can be substituted at different positions in the polymers. For instance, exchanging into the polymer chains, reside at the amorphous/crystalline boundaries and form charge transfer junctions, or form ion aggregates between the polymer chains [21].

In our previous works [22,23], dielectric, optical, electrical, structural, morphological, and chemical properties of PEO complexed with molecular iodine (I_2) with a concentration of I_2 ranged from 1 to 7 wt% were investigated. We concluded that complexed PEO with I_2 with concentrations between 0 and 7% decreases the bandgap energy from 4.42 to 3.28 eV in addition to increasing the electrical conductivity from 20 pS/cm to 120,000 pS/cm. This work aims to investigate the effect of low doping levels of molecular iodine in PEO on the optical, dielectric, and electrical properties of PEO/I_2 complex composite films. In addition, the doping mechanism and the charge transfer mechanism were also investigated using different spectroscopic techniques. The relationship between the doping mechanism, structural properties with other physical properties were studied accordingly.

2. Experimental sections

2.1. Sample preparation

Polyethylene oxide (PEO) ($–CH_2CH_2O–)_n$ with M_w 300,000 g/mol, iodine (I_2) with M_w 126.90 g/mol, and methanol (CH_4O) with M_w 32.04 g/mol were obtained from Sigma-Aldrich, while PTFE (polytetrafluoroethylene) substrate was sourced from RCT Reichelt Chemietechnik GmbH. For optical characterizations, a polymeric stock solution of PEO in methanol was synthesized by dissolving 1.0 g PEO in 100 mL of methanol at 45 °C. In addition, the stock solution of I_2 in methanol was prepared by dissolving 0.1 g of I_2 in 100 mL of methanol. Later, the complex composite solutions with concentrations of 0, 0.01, 0.03, 0.06, 0.1, and 1 wt% were prepared by mixing 20 mL PEO/methanol polymer solution with the calculated amount of I_2/methanol stock solution (Table 1). PEO/I_2/methanol composite solutions were repeatedly mixed using continuous magnetic string and ultrasonic water bath. PEO/I_2 composite films were prepared using a dip-coating technique for 2 h. The films were dried for 24 h at ambient temperature and pressure. The films thickness was determined using Q. Al Bataineh et al. mathematical model, that proposed the fit function between the transmission spectra as a function of the incident photon wavelength (Table 1) [24,25].

For dielectric characterizations, a polymeric stock solution of PEO in methanol was synthesized by dissolving 0.5 g PEO in 5 mL of methanol at 45 °C using continuous magnetic stirring for 5 h. In addition, the stock solution of I_2 in methanol was prepared by dissolving 10 mg I_2 in 5 mL methanol. Later, the complex composite solutions with concentrations of 0, 0.01, 0.03, 0.06, 0.1, and 1 wt% were prepared by mixing 0.5 mL PEO/methanol polymer solution with the calculated amount of I_2/methanol stock solution (Table 2). PEO/I_2/methanol composite solutions were repeatedly mixed using continuous magnetic string and ultrasonic water bath. PEO/I_2 composite films were casting on PTFE substrates using an adapted spin coater at low speed to avoid splattering of the solution form the substrate. The films were dried for 24 h at ambient temperature and pressure. Finally, the composite films were smoothly peeled from the PTFE substrate. Brunswick Instrument was used to measure the film thickness (Table 2).

2.2. Sample characterizations

Crystal and chemical properties of PEO/I_2 composite films were studied using X-ray diffraction (XRD, Rigaku Ultima IV), Fourier transform infrared spectroscopy (FTIR Microscope HYPERION 3000 from Bruker), HN MAS NMR (600.13 MHz, Bruker AVIII-600 spectrometer), and UV–Vis spectrophotometer (U–3900H). UV–Vis spectrophotometer (U–3900H) with a total internal reflectance sphere was used to measure the transmittance (T%) and reflectance (R%) spectra in the (250 nm–700 nm) spectral range. Other related optical parameters, such as refractive index (n) and extinction coefficient (k) are calculated by $n = (1 + R/1 - R) + \sqrt{(4R/(1-R)^2) - k^2}, k = \alpha\lambda/4\pi$ [26]. Bandgap energy and Urbach energy are calculated using Q. Al Bataineh et al. model [24,25], Urbach empirical rule [27], respectively,

$$T(E) = e^{-\frac{4\pi dE}{hc}\frac{A(E-E_g)^2}{E^2-BE+C}} \quad (1)$$

$$\alpha = \alpha_0 \exp(h\nu / E_U) \quad (2)$$

The dielectric loss ε'' of PEO/I_2 complex composite films at different temperatures ranging from 298 K to 318 K is measured using a broadband dielectric spectrometer (Alpha-A Novocontrol GmbH) in the 0.1 Hz–10^7 Hz region. Havriliak-Negami (HN) model was used to analyze the ε''-spectra. The ε''-spectra is found to have α-relaxation peak (first term in Equation (1)) in addition to the conductivity (third term in Equation (1)), while the β-relaxation peak (second term in Equation (1)) is not present in our data [28]:

$$\varepsilon'' = \Delta\varepsilon_1 \frac{\sin\gamma_1\left(\arctan\left\{\frac{(\omega\tau)^{1-\alpha_1}\cos\left[\frac{\pi}{2}\alpha_1\right]}{1+(\omega\tau)^{1-\alpha_1}\sin\left[\frac{\pi}{2}\alpha_1\right]}\right\}\right)}{\left\{1+2(\omega\tau)^{1-\alpha_1}\sin\left[\frac{\pi}{2}\alpha_1\right]+(\omega\tau)^{2(1-\alpha_1)}\right\}^{\gamma 1/2}} + \Delta\varepsilon \frac{\sin\gamma\left(\arctan\left\{\frac{(\omega\tau)^{1-\alpha}\cos\left[\frac{\pi}{2}\alpha\right]}{1+(\omega\tau)^{1-\alpha}\sin\left[\frac{\pi}{2}\alpha\right]}\right\}\right)}{\left\{1+2(\omega\tau)^{1-\alpha}\sin\left[\frac{\pi}{2}\alpha\right]+(\omega\tau)^{2(1-\alpha)}\right\}^{\gamma/2}} + \left(\frac{\sigma}{2\pi\omega\varepsilon_0}\right)^N \quad (3)$$

where $\Delta\varepsilon$ is the dielectric strength, τ is the relaxation time, σ is the electrical conductivity, N is an exponent that characterizes the conduction process, and ε_0 is the permittivity of vacuum. The exponents α

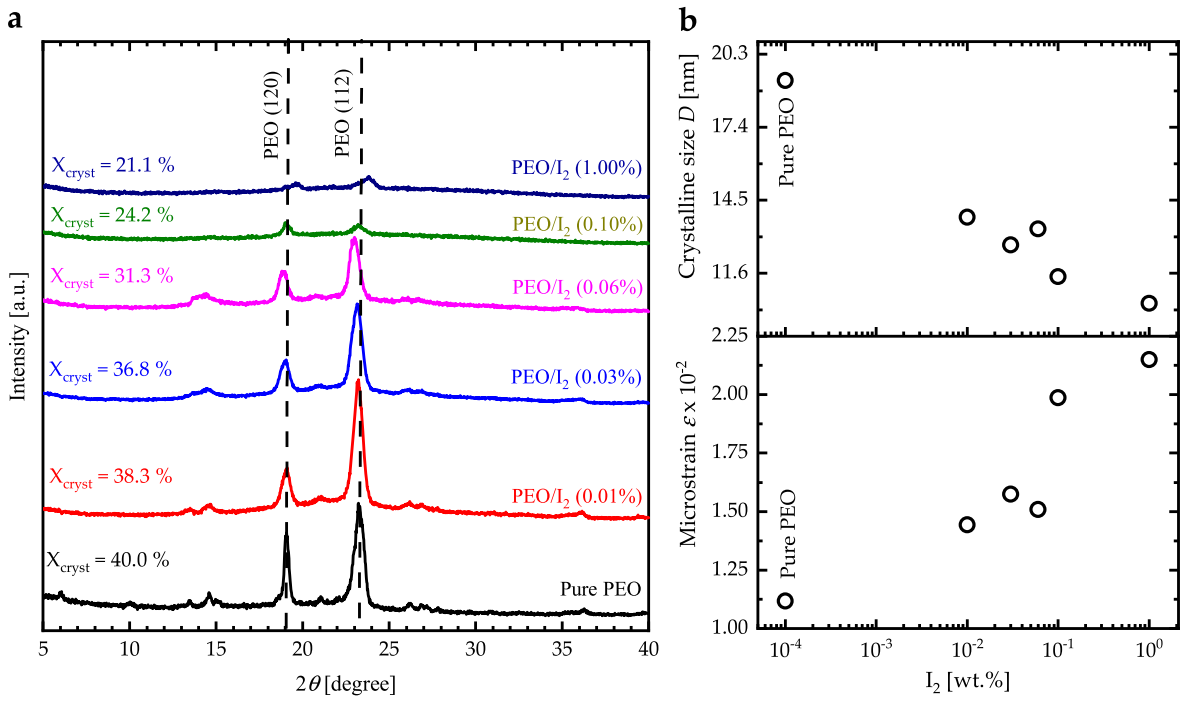

Fig. 1. **(a)** XRD patterns of pure PEO and PEO/I_2 complex composite films, **(b)** Crystalline size and strain for PEO/I_2 complex composite films as a function of I_2 concentrations.

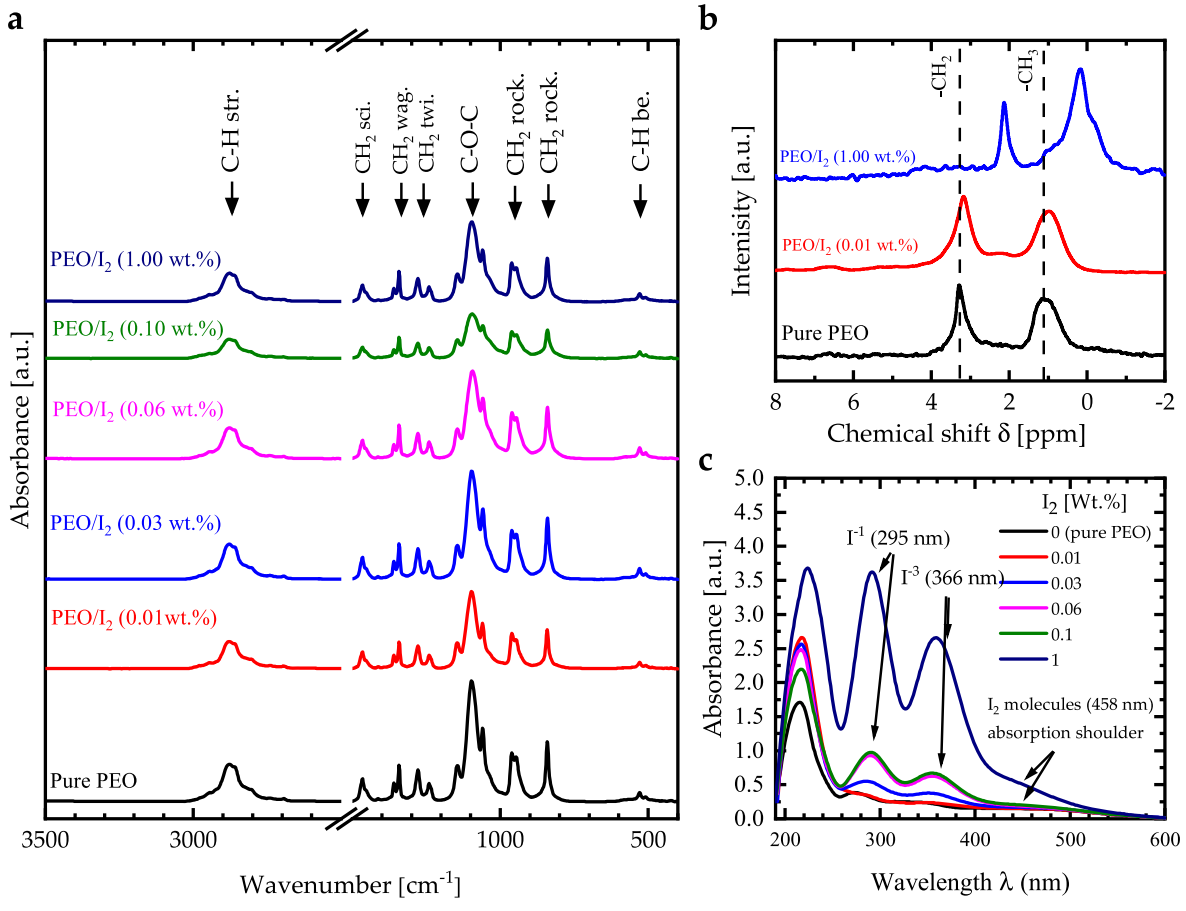

Fig. 2. **(a)** FTIR spectra, **(b)** ^{1}H NMR spectra, **(c)** UV–Vis absorbance spectra of PEO/I_2 complex composite films.

and β are the HN fitting parameters describing the asymmetric and broadening parameters of the relaxation peaks, respectively.

3. Results and discussion

3.1. Crystal structural characterization

The crystallinity of the complex composite films of pure PEO and PEO/I_2 with different concentrations of I_2 is studied by employing XRD technique using CuKα ray with a wavelength of 0.1540598 nm. The obtained XRD patterns are shown in Fig. 1a. The peaks of PEO are observed at diffraction angles of 19.08° and 23.26°, representing PEO crystallographic planes of 120 and 112, respectively [29,30]. PEO/I_2 complex composite films show the same XRD spectrum with slight shifts in the peaks position and an apparent reduction in intensities. The decrease in intensity and the shift in peaks positions are attributed to the increase in the amorphous nature of the films and the increase in the strain induced in their structure. This can be attributed to that the interaction between molecular iodine with PEO through charge transfer mechanism leads to the structural disruption of PEO matrix, which reduces the intermolecular interactions in the crystal phase of PEO [31]. In addition, the crystallinity degree ($X_{cryst} = 100\% \times A_{cryst}/(A_{cryst} + A_{amorph})$) was calculated for all samples (Fig. 1a). The crystallinity degree decreases continuously from 40.0% for pure PEO to 21.1% for PEO/I_2 (1.0%)

The crystallite size (D) of the film microstructure of PEO/I_2 planes is obtained using Scherer formula $D = k\lambda/\beta_{2\theta}\cos\theta$ [32], where k is 0.9, λ is X-ray wavelength and $\beta_{2\theta}$ is FWHM of PEO–I_2 peaks in radians. Moreover, the strain (ε) is calculated by $\varepsilon = \beta_{2\theta}\cos\theta/4$ [33]. Fig. 1b shows the calculated average crystallite size (D) and average strain (ε). The strain of PEO/I_2 films increases and the crystallite size decreases as the I_2 concentration is increased in the PEO matrix. These changes enhance the amorphous nature in the complex composite films revealing a good interaction between the I_2 and PEO polymer.

3.2. Chemical structure characterizations

Iodine ionization and complexation with PEO are studied using FTIR, NMR, and UV–Vis absorption spectroscopies. The vibrational bands of the PEO/I_2 complex composite films are investigated by FTIR spectroscopy (Fig. 2a). The FTIR spectra show the typical vibrational bands of PEO. The vibrational band observed at 2880 cm^{-1} represents the C–H bond stretching. The band at 1466 cm^{-1} is associated with the CH_2 bond scissoring. The band at 1340 cm^{-1} characterizes the CH_2 bonds wagging. The two bands observed at 1276 cm^{-1} and 1235 cm^{-1} are assigned to the CH_2 bonds twisting. The two bands located at 955 cm^{-1} and 840 cm^{-1} label the CH_2 bonds rocking. At 527 cm^{-1}, a band is observed to be related to the C–H bonds bending. Moreover, the triplet peak of the C–O–C stretching band at a maximum of 1088 cm^{-1} confirms the semicrystalline phase of PEO [34]. It can be seen that apparent changes in linewidth and peak position are observed with increasing I_2 concentration. This can be attributed to the electronegativity difference between iodine and PEO atoms [18]. Likewise, the change in intensity, linewidth, and band position of the triplet peak of the C–O–C stretching band confirms the change in the degree of crystallinity [34].

^{1}H NMR spectra of pure PEO and PEO/I_2 complex composite films with selected I_2 concentrations show two major peaks at 1.038 ppm and 3.224 ppm, representing the amorphous phase and crystal phase, respectively (Fig. 2b) [35]. The amorphous phase peak has a symmetric shape at room temperature, while the NMR peak of the crystalline is still a broad asymmetric convoluted peak indicating that the crystalline phase is still in the rigid glassy form. Introducing I_2 into the PEO matrix leads to a shift of the peak to the lower chemical shifts indicating that the protons in PEO have a higher electron density. This means that I_2 is acting as a Lewis acid, and PEO is acting as Lewis bases, hence, molecular iodine reacts favorably with PEO molecules through a charge transfer mechanism, to form charge transfer complexes (CTCs) as confirmed by electron spin resonance spectroscopy [23].

The absorbance spectra of PEO/I_2 complex composite films with I_2 concentrations of wt.% = 0, 0.01, 0.03, 0.06, 0.1 and 1 are shown in Fig. 2c. The addition of I_2 causes a significant shift of the absorbance band edge to a higher wavelength region and therefore a redshift in the optical bandgap is obtained, which can be attributed to the oxidation interactions between the PEO as a cation and the iodine anion, which forms polarons in the band structure and consequently shifting the absorbance band edge to a higher wavelengths [2].

The absorbance spectra of PEO/I_2 complex composite films exhibit three transition bands with maxima at around 220, 277, and 349 nm, respectively. These three transitions maybe related to polyenic domains composed of PEO bonds [36]. According to molecular orbital theory [37], there are three possible electronic transitions for PEO. The first transition appears at 5.64 eV (220 nm) and can be attributed to $\pi\rightarrow\pi^*$ electronic transition originating from unsaturated bonds [38]. The second appears at 4.48 eV (277 nm) and can be assigned to $n\rightarrow\pi^*$ electronic transition originating from carbonyl C–O bonds [39]. The third transition appears at 3.55 eV (349 nm) attributed to the $n\rightarrow\sigma^*$ transition originating from C–H bond. The intensity of the three absorbance bands increases as the iodide concentration in the PEO matrix is increased. Moreover, an absorption shoulder appears at 458 nm maybe attributed to the absorption of charge transfer complex formation between PEO and I_2 [40,41]. In PEO/I_2 complex composites, the absorption peaks at 295 and 366 nm are associated with the iodide (I^-) and triiodide (I_3^-) absorption, respectively [42]. The iodide (I^-) and triiodide (I_3^-) molecules formation within the PEO matrix represents the interaction between the PEO and I_2. The negative charge of iodine molecules transferred to the PEO matrix as given by Refs. [43,44],

$$I_2 + 2e^- \leftrightarrow I^- + I^- \quad (4)$$

$$I^- + I_2 \leftrightarrow I_3^- \quad (5)$$

3.3. Optical characterizations

The refractive index spectra (n) of PEO/I_2 complex composite films are shown in Fig. 3a. In the low wavelength range ($\lambda < 350\ nm$) for PEO film and ($\lambda < 450\ nm$) for PEO–I_2 films, n spectra show anomalous dispersion indicating many photon-matter interactions such as, photon absorption due to the $\pi - \pi^*$ electronic transition, photon dispersion, and the resonance effect resulting from the equality of the incident photon frequency and the plasma frequency [45,46]. In the high wavelength range, n spectra exhibit normal dispersion behavior. It continuously decreases as the wavelength is increased. For PEO films, n values vary from 1.66 to 2.00. Furthermore, it increases as the concentration of I_2 in the polymeric matrix is increased to wt.% = 1%. This increase may be attributed to the condensation of iodine ions to polyiodide [47]. Fig. 3b shows the extinction coefficient spectra (k) of PEO/I_2 complex composite films. Prior to the absorption edge, k decreases drastically for incident photons having wavelengths shorter than those in the visible region. The PEO film transmits photons in the visible region without a decay or attenuation because there are no free electrons in the PEO matrix. Ejection of strongly bounded electrons in the PEO matrix and transporting them into the conduction band requires high incident photon energy (UV-light). Moreover, k values increase when I_2 content in PEO films is increased. This indicates that incorporation of I_2 into PEO films results in increasing the light energy loss since I_2 molecules contain free electrons that can absorb incident lower energy photons and consequently transport them into higher energy [48,49]. The small peak in the k spectra of the PEO/I_2 films located 350 nm and 450 nm is due to the transition from X to B band of I_2 [50].

Fig. 3c shows the variation of bandgap energy and Urbach energy of PEO/I_2 complex composite films as a function of I_2 concentration. The bandgap of the PEO film is found to be 4.42 eV. Introducing 0.01 wt% of

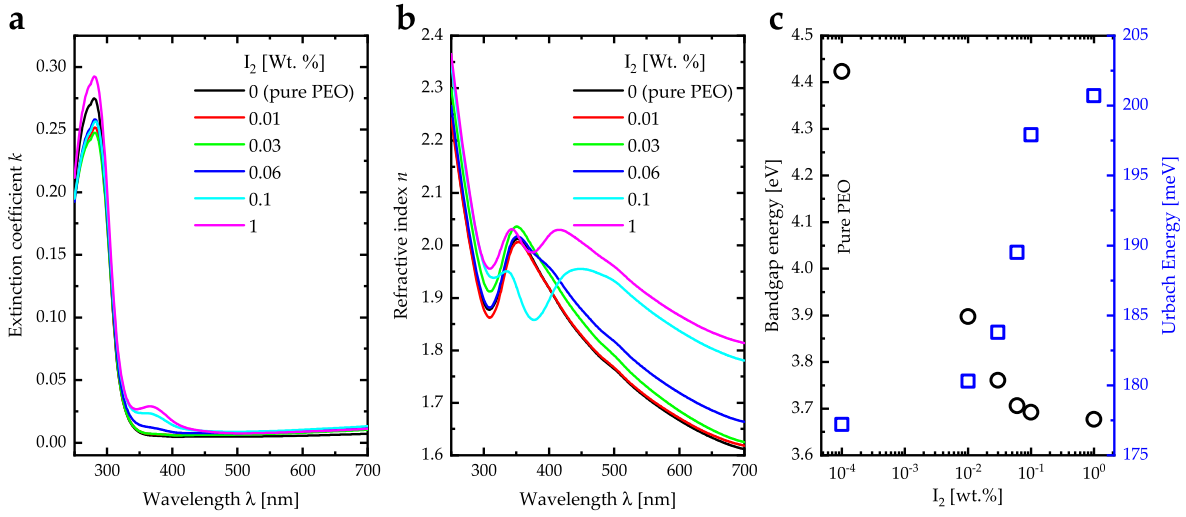

Fig. 3. (a) Refractive index spectra *n*, **(b)** Extinction coefficient spectra *k* of PEO/I_2 complex composite films for different I_2 concentrations. **(c)** Band gap energies (E_g) and Urbach energies (E_U) of PEO/I_2 complex composite films as a function of I_2 concentrations.

I_2 into the PEO matrix reduces the bandgap sharply to 3.90 eV. A further increasing of I_2 concentration up to 1.0 wt% decreases the bandgap energy to 3.68 eV. The interaction between PEO and I_2 is an oxidative interaction indicating that the radical cation in the PEO is formed with the iodine anion and consequently forms polarons between the valence and conduction bands and decreases the energy bandgap [2]. The Urbach energy of PEO film is 177.2 meV. It continuously increases as I_2 concentration is increased incrementally into PEO matrix. This behavior is a clear signature of increasing the disorder and the strain in the investigated PEO/I_2 films [51]. This finding is in good agreement with the results obtained from the XRD investigations (section 3.1).

3.4. Dielectric relaxation

To clarify the HN fitting function, ε'' spectra of pure PEO film at two different temperatures (288 K and 318 K) are shown in Fig. 4. The figure shows the regions of the α-relaxation peak (α-relaxation is associated with the local segmental motions of amorphous parts in the polymer chain) and the electrical conductivity part [7]. The figure illustrates the measured ε'' spectra of PEO (black circles), conductivity contribution (green line), α-relaxation (blue line), and HN fitting function (red line) at temperatures of 288 K and 318 K. The HN function is the only proper function to describe the ε'' spectra in the wide frequency range [28].

Fig. 5(a–f) depicts the ε'' spectra of the PEO/I_2 complex composite films (I_2 = 0, 0.01, 0.03, 0.06, 0.1 and 1.0 wt%) for different temperatures fitted using HN model (Equation (1)). ε'' variation clarifies the energy required to tune the dipoles in the field directly with changing frequency, temperature, and iodine doping concentration [52]. It is worth discussing ε''-relaxation at different temperatures and iodine doping concentrations as a function of frequency. In the low-frequency range, the polarization of the electrode predominates that leads to ion accumulation at the interface between the electrode and the polymer [53]. In the high-frequency range, the applied field originates an opposite environment at the composite for dipole adjustment. This behavior maybe attributed to the accumulation of dipoles because of the absence of the required rotation/orientation period. Increasing

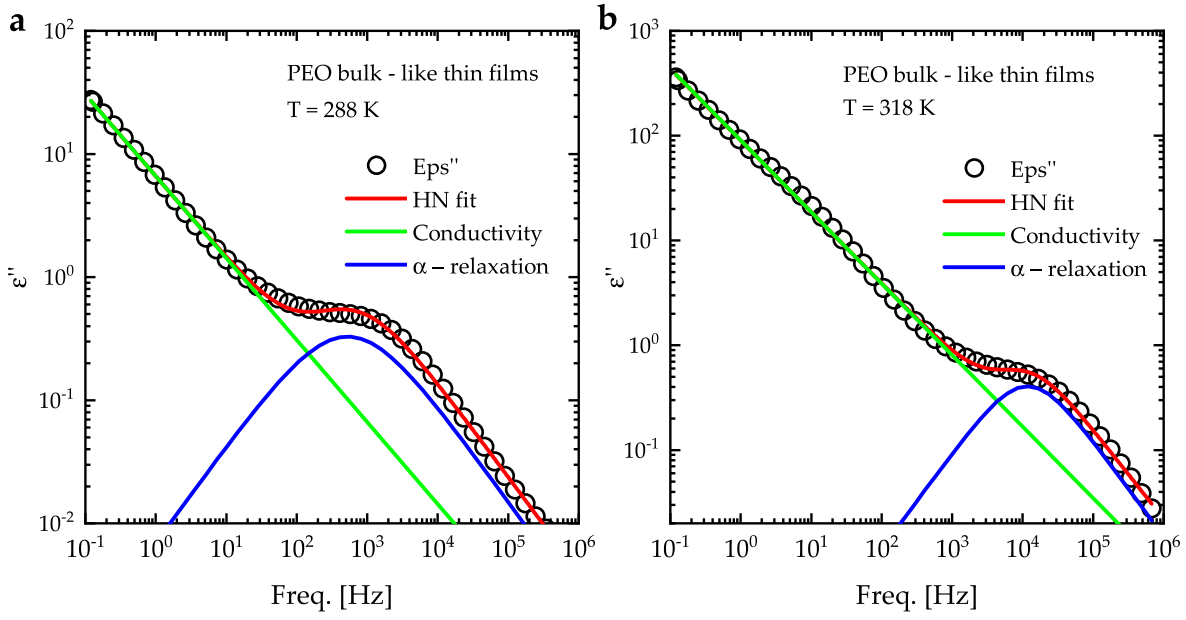

Fig. 4. HN function components α-relaxations with addition to $(\sigma_{dc}/\varepsilon_0\omega)^N$) contributions signifying quantitatively the experimental dielectric loss (ε'') of PEO at **(a)** 288 K and **(b)** 318 K.

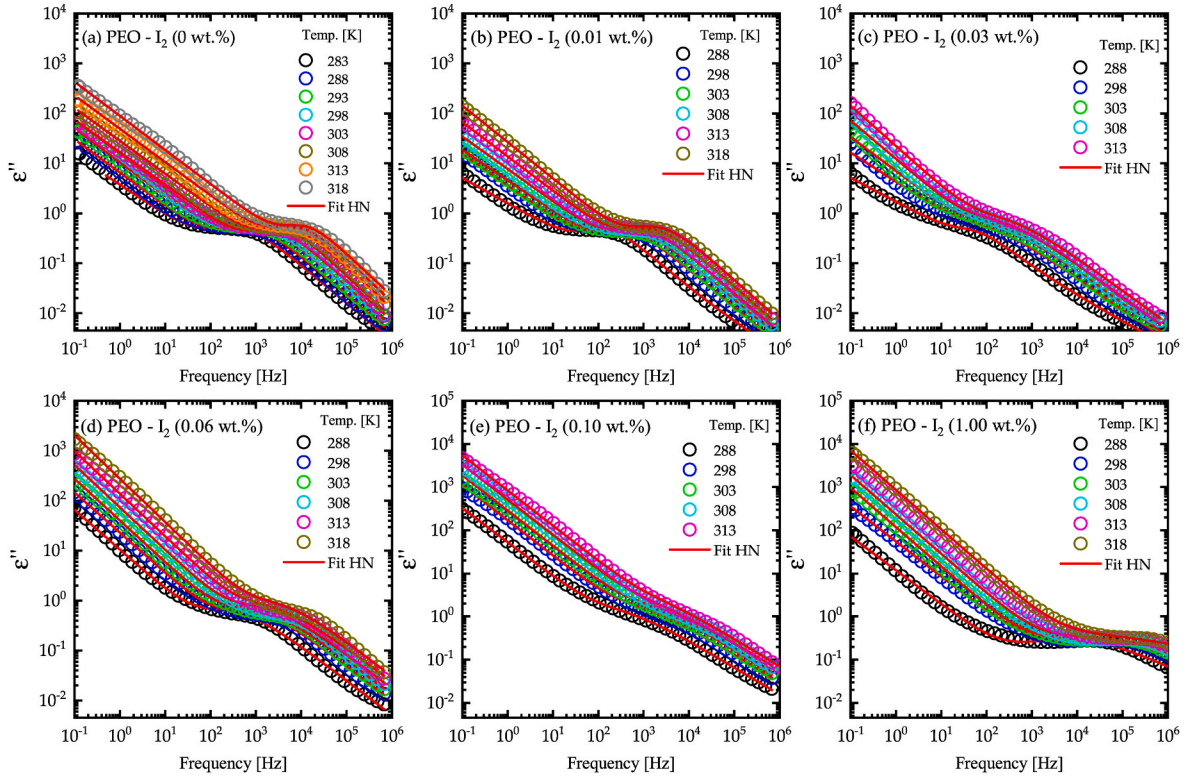

Fig. 5. Experimental ε" of PEO/I_2 composite films at different I_2 concentrations in addition to HN fitting function **(a)** pure PEO, **(b)** 0.01 wt%, **(c)** 0.03 wt%, **(d)** 0.06 wt%, **(e)** 0.1 wt% and **(f)** 1.0 wt% versus frequency at different temperatures.

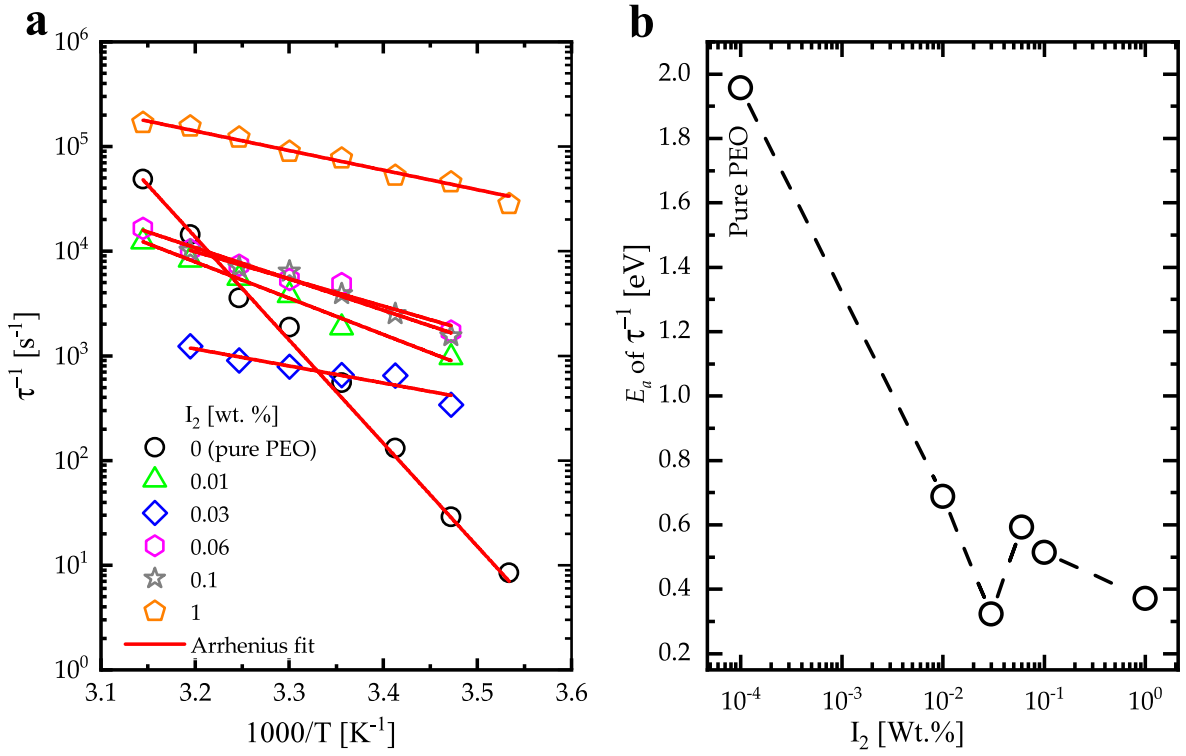

Fig. 6. **(a)** The τ_{HN}^{-1} values for PEO/I_2 complex composite films versus 1000/T (K^{-1}) for α-relaxation process, and **(b)** the activation energies deduced from τ_{HN}^{-1}.

dielectric constant values increases the ionic conductivity [54–56]. The loss distribution at high temperatures in the high-frequency range is attributed to thermal vibrational activation in the composite films. Also, the composite films do not have enough time to interact with the applied electric field. Furthermore, ε'' values of PEO/I_2 composite film results from molecular dipole motion and space charge migration [57]. Moreover, the dielectric properties of the PEO/I_2 composite films are related to the intermolecular force between the space charge polarization and

polymer matrix at amorphous/crystalline interface [58]. At high temperature, the intermolecular forces dissociates converting the polymer from viscoelastic phase to rubbery phase, and consequently increases the freedom of segmental motion. This decreases the amount of dissipated energy dispersed [59]. At low temperatures, the dielectric constant decreases due to the reduction of the freedom of the segmental motion [60].

By fitting ε'' spectra as a function of frequency using HN model at T 280 K, one can get the following parameters: dielectric strength ($\Delta\varepsilon$), relaxation time (τ), electrical conductivity (σ). In addition, other parameters like α, β, and N have been obtained for α-relaxation processes above T_g of PEO ($\simeq$ 215 K). The ε'' values increase and shift toward high frequency as the temperature increases. At constant T, the magnitude of the dielectric loss increases as the frequency decreases [61–63].

3.3.1. Relaxation time (τ)

Fig. 6a shows the variation of the inverse of dielectric relaxation time (τ_{HN}) deduced from HN fitted ε" as a function of (1000/T (K^{-1})). The inverse of τ_{HN} can be fitted using Arrhenius function for all samples indicating that the samples are thermally activated. Moreover, the relaxation times increase as the temperature is increased. This can be interpreted in terms of the incremental increase in the freedom of segmental motion connected with the iodine ions, and consequently, an enhancement in the ionic transport properties of the composite films. Arrhenius-like behavior for τ^{-1} can be defined as $\tau^{-1} = \tau_0^{-1}\exp(-E_a/K_BT)$, where E_a is the activation energy [64]. Fig. 6b shows the calculated activation energy E_a as a function of I_2 concentrations. It can be seen that the activation energy decreases as I_2 concentration is increased.

3.3.2. Dielectric strength ($\Delta\varepsilon$)

Fig. 7a illustrate the dielectric relaxation strength ($\Delta\varepsilon$) of PEO/I_2 complex composite films versus (1000/T (K^{-1})). It is clear that $\Delta\varepsilon$ increases as the temperature is increased indicating that the PEO bulk-like thin film is dominated by the amorphous phase. The temperature-dependence of $\Delta\varepsilon$ follows Arrhenius-like behavior for all samples (Fig. 7a). Arrhenius-like behavior for $\Delta\varepsilon$ can be defined as $\Delta\varepsilon = \Delta\varepsilon_0\exp(-E_a/K_BT)$, where $\Delta\varepsilon_0$ is the pre-exponential factor. The activation energy that are deduced from $\Delta\varepsilon$ show maximum value at 0.03% of I_2 dopant concentration (Fig. 7b). This agrees with the activation energy values deduced from the relaxation time. The $\Delta\varepsilon$ shows a maximum at 0.1 wt% of I_2 (Fig. 7c) for all temperatures indicating an invariance in the dissociation and dynamicity mechanism.

3.3.3. Electrical conductivity

Fig. 8a illustrate the electrical conductivity (σ) of PEO/I_2 complex composite films versus (1000/T (K^{-1})) fitted to Arrhenius function. Arrhenius-like behavior of σ can be defined as $\sigma = \sigma_0\exp(-E_a/K_BT)$, where σ_0 is the pre-exponential factor with the dimension of (ps/cm). Activation energies deduced from σ decreases as I_2 concentration are increased (Fig. 8b), and consequently, the electrical conductivity is increased. The activation energy values deduced from σ show a minimum value at 0.03 wt% of I_2 (Fig. 8b). This means that the charge carrier's migration takes place because of the formation/breaking the coordinating sites in polymer matrix.

Fig. 8c illustrate the electrical conductivity (σ) of PEO/I_2 complex composite films versus I_2 [wt.%] at selected temperatures (288, 298, 303, 308) K. Increasing I_2 concentration up to 0.1 wt% induces a rapid increase in the σ. It then decreases slightly as I_2 concentration increases up to 1 wt%, due to ionization of iodine. Accordingly, the iodide (I^-) is the dominant anion in PEO/I_2 composite films compared to triiodide (I_3^-) and polyiodide. In addition, at 1 wt% of I_2, I_3^- are formed in the composite according to equation (3). Moreover, the electrical conductivity increases by increasing temperature results from the thermal activation of coexisting operations in the composite films, such as electron hopping, enhancing ions mobility, depolarization of the relaxation process [65].

4. Conclusions

In conclusion, the effect of low concentrations of I_2 doping in PEO films was investigated by employing different spectroscopic techniques. The difference in the electronegativity between PEO atoms and iodine in addition to charge transfer interaction leads to FTIR and NMR peaks' position shifts and their intensities change due to the incorporation of I_2 into the PEO matrix. In addition, the charge transfer interaction between PEO and molecular iodine and its ions leads to structural disruption of PEO matrix, which reduces the intermolecular interactions in the crystal phase of PEO, and consequently decreases the crystallinity degree of the composite. The UV–Vis absorption spectrum of PEO/I_2 composites shows four absorbance bands at around 220 nm, 290 nm, 360 nm, and 440 nm indicating the absorption of charge transfer complex formation between PEO and I_2, iodide, tri-iodides, and molecular iodine, respectively. The optical band gap energy decreases from 4.42 eV to 3.678 eV as I_2 content increases from 0 to 1 wt%. Moreover, the refractive index increases as the concentration of I_2 increases in the polymer matrix. Furthermore, the relaxation time behavior at T < T_g of PEO/I_2 composite films may be attributed to a combined effect of the temperature-

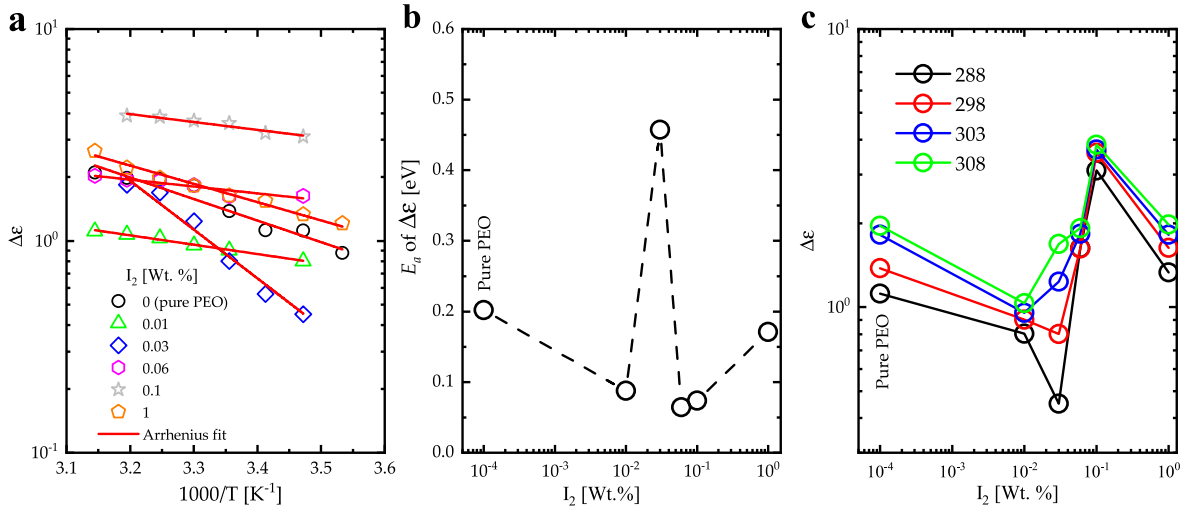

Fig. 7. (a) The $\Delta\varepsilon$ values of PEO/I_2 complex composite films versus 1000/T (K^{-1}) for α-relaxation process, **(b)** the activation energies deduced from $\Delta\varepsilon$, and (c) The $\Delta\varepsilon$ values of PEO/I_2 complex composite films at different temperatures versus I_2 [wt.%].

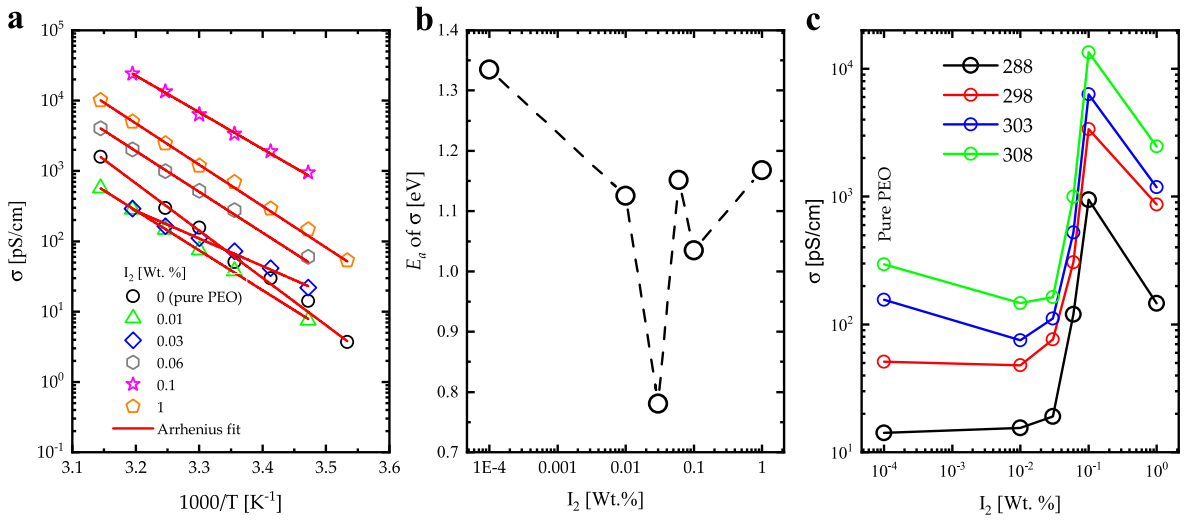

Fig. 8. **(a)** The σ PEO/I_2 complex composite films versus 1000/T (K^{-1}) for α-relaxation process, **(b)** the activation energies deduced from σ, and (c) the σ values for PEO/I_2 complex composite films at different temperatures versus I_2 [wt.%].

dependent dielectric relaxation time and to interfacial/electrode space-charge polarizations. In addition, the ionic concentrations dominate the relaxation time due to the favorable I^{-3}-polymer clustering. The conductivity curves show a maximum for I_2 concentration of 0.1%. At 1% of I_2 concentration, the conductivity decreases slightly. This can be interpreted in terms of increased amorphous phase due to the incorporation of I_2 in the polymer electrolytes. The decrease in the electrical conductivity between 0.1% and 1% I_2 concentrations can be attributed to the ionic iodine clustering. Manipulation of chemical, optical, electrical, structural and dielectric properties of PEO/I_2 complex composite films by low doping and variation of temperature yields nanocomposites that could be potential candidates for optical and optoelectronic applications.

Author contributions

Conceptualization, A.T., Q.B. and B.S.; methodology, Q. B, A.A. A. S…; software, A.T. and R.S.; validation, A.T. and R.S..; formal analysis, Q.B. and B.S.; investigation, A.A. and A.S.; resources, A.T. and R.S.; data curation, Q.B. and A.A.; writing—original draft preparation, A.T. and Q. B.; writing—review and editing, A.A., A.S., B.S. and R.S.; visualization, Q.B. and A.T.; supervision, A.T. and R.S.; project administration, A.T. and R.S. All authors have read and agreed to the published version of the manuscript.

Declaration of competing interest

The authors declare that they have no known competing financial interests or personal relationships that could have appeared to influence the work reported in this paper.

Data availability

Data will be made available on request.

Acknowledgment

Financial Support by the Ministerium für Innovation, Wissenschaft und Forschung des Landes Nordrhein-Westfalen, the Senatsverwaltung für Wirtschaft, Technologie und Forschung des Landes Berlin, and the Bundesministerium für Bildung und Forschung is gratefully acknowledged. R.S. work is supported by NSF (award # 2044049).

References

[1] M.A. AL-Akhras, S.E. Alzoubi, A.A. Ahmad, R. Ababneh, A. Telfah, Studies of composite films of polyethylene oxide doped with potassium hexachloroplatinate, J. Appl. Polym. Sci. 138 (5) (2021), 49757.
[2] A. Telfah, M.-A. Al-Akhras, K.A. Al-Izzy, A.A. Ahmad, R. Ababneh, M.J.A. Ahmad, C.J. Tavares, R. Hergenröder, Dielectric relaxation, XPS and structural studies of polyethylene oxide/iodine complex composite films, Polym. Bull. (2021) 1–20.
[3] A. Abdelghany, A. Oraby, M. Farea, Influence of green synthesized gold nanoparticles on the structural, optical, electrical and dielectric properties of (PVP/SA) blend, Phys. B Condens. Matter 560 (2019) 162–173.
[4] A.-T. Mohammed, A.T. Mou'ad, M. Owaidat, A. Monther, Optical Characterization of Thin Films Poly (Ethylene Oxide) Doped with Cesium Iodide, 2018.
[5] S.B. Aziz, R.B. Marif, M. Brza, A.N. Hassan, H.A. Ahmad, Y.A. Faidhalla, M. Kadir, Structural, thermal, morphological and optical properties of PEO filled with biosynthesized Ag nanoparticles: new insights to band gap study, Results Phys. 13 (2019) 102220.
[6] D. Bresser, S. Lyonnard, C. Iojoiu, L. Picard, S. Passerini, Decoupling segmental relaxation and ionic conductivity for lithium-ion polymer electrolytes, Molecular Systems Design & Engineering 4 (4) (2019) 779–792.
[7] A. Telfah, M.M. Abdul-Gader Jafar, I. Jum'h, M.J.A. Ahmad, J. Lambert, R. Hergenröder, Identification of relaxation processes in pure polyethylene oxide (PEO) films by the dielectric permittivity and electric modulus formalisms, Polym. Adv. Technol. 29 (7) (2018) 1974–1987.
[8] E. Abdallah, T.F. Qahtan, E. Abdelrazek, G. Asnag, M. Morsi, Enhanced the structural, optical, electrical and magnetic properties of PEO/CMC blend filled with cupper nanoparticles for energy storage and magneto-optical devices, Opt. Mater. 134 (2022) 113092.
[9] A. Karmakar, A. Ghosh, Dielectric permittivity and electric modulus of polyethylene oxide (PEO)–LiClO4 composite electrolytes, Curr. Appl. Phys. 12 (2) (2012) 539–543.
[10] Z. Xue, D. He, X. Xie, Poly (ethylene oxide)-based electrolytes for lithium-ion batteries, J. Mater. Chem. 3 (38) (2015) 19218–19253.
[11] E.M. Abdelrazek, A.M. Abdelghany, S.I. Badr, M.A. Morsi, Structural, optical, morphological and thermal properties of PEO/PVP blend containing different concentrations of biosynthesized Au nanoparticles, J. Mater. Res. Technol. 7 (4) (2018) 419–431.
[12] M. Farea, A. Abdelghany, M. Meikhail, A. Oraby, Effect of cesium bromide on the structural, optical, thermal and electrical properties of polyvinyl alcohol and polyethylene oxide, J. Mater. Res. Technol. 9 (2) (2020) 1530–1538.
[13] M. Farea, A. Abdelghany, A. Oraby, Optical and dielectric characteristics of polyethylene oxide/sodium alginate-modified gold nanocomposites, RSC Adv. 10 (62) (2020) 37621–37630.
[14] A. Migdadi, A.A. Ahmad, A.M. Alsaad, Q.M. Al-Bataineh, A. Telfah, Electrical and thermal characterizations of synthesized composite films based on polyethylene oxide (PEO) doped by aluminium chloride (AlCl3), Polym. Bull. (2022) 1–14.
[15] Q.M. Al-Bataineh, A.A. Ahmad, A.M. Alsaad, A. Migdadi, A. Telfah, Correlation of electrical, thermal, and crystal parameters of complex composite films based on polyethylene oxide (PEO) doped by copper sulfate (CuSO4), Phys. B Condens. Matter 645 (2022) 414224.
[16] J.-L. Bredas, B. Thémans, J. Fripiat, J.-M. André, R. Chance, Highly conducting polyparaphenylene, polypyrrole, and polythiophene chains: an ab initio study of the geometry and electronic-structure modifications upon doping, Phys. Rev. B 29 (12) (1984) 6761.
[17] S. Chand, N. Kumar, Effect of iodine doping on electrical conduction in PVB films, J. Mater. Sci. Lett. 8 (9) (1989) 1009–1010.

[18] K. Bazaka, M.V. Jacob, Effects of iodine doping on optoelectronic and chemical properties of polyterpenol thin films, Nanomaterials 7 (1) (2017) 11.
[19] L. Dai, A.W. Mau, H.J. Griesser, D. Winkler, T.H. Spurling, X. Hong, Y. Yang, J. W. White, I2-Doping" of 1, 4-polydienes, Synth. Met. 69 (1–3) (1995) 563–566.
[20] A. Abu-Jamous, A.M. Zihlif, Study of the electrical conduction in poly (ethylene oxide) doped with iodine, Phys. B Condens. Matter 405 (13) (2010) 2762–2767.
[21] G. Palácio, S.H. Pulcinelli, R. Mahiou, D. Boyer, G. Chadeyron, C.V. Santilli, Coupling photoluminescence and ionic conduction properties using the different coordination sites of ureasil–polyether hybrid materials, ACS Appl. Mater. Interfaces 10 (43) (2018) 37364–37373.
[22] A. Telfah, M.-A. Al-Akhras, K.A. Al-Izzy, A.A. Ahmad, R. Ababneh, M.J.A. Ahmad, C.J. Tavares, R. Hergenröder, Dielectric relaxation, XPS and structural studies of polyethylene oxide/iodine complex composite films, Polym. Bull. 79 (6) (2022) 3759–3778.
[23] A. Telfah, Q.M. Al-Bataineh, E. Tolstik, A.A. Ahmad, A.M. Alsaad, R. Ababneh, C. J. Tavares, R. Hergenröder, Optical, electrical and chemical properties of PEO: I2 complex composite films, Polym. Bull. (2022) 1–15.
[24] Q.M. Al-Bataineh, A. Alsaad, A. Ahmad, A. Telfah, A novel optical model of the experimental transmission spectra of nanocomposite PVC-PS hybrid thin films doped with silica nanoparticles, Heliyon 6 (6) (2020) e04177.
[25] Q.M. Al-Bataineh, A.A. Ahmad, A. Alsaad, A.D. Telfah, Optical characterizations of PMMA/metal oxide nanoparticles thin films: bandgap engineering using a novel derived model, Heliyon 7 (1) (2021) e05952.
[26] A. Ahmad, A. Alsaad, Q. Al-Bataineh, M. Al-Naafa, Optical and structural investigations of dip-synthesized boron-doped ZnO-seeded platforms for ZnO nanostructures, Appl. Phys. A 124 (6) (2018) 458.
[27] Q.M. Al-Bataineh, M. Telfah, A.A. Ahmad, A.M. Alsaad, I.A. Qattan, H. Baaziz, Z. Charifi, A. Telfah, Synthesis, crystallography, microstructure, crystal defects, optical and optoelectronic properties of ZnO: CeO2 mixed oxide thin films, in: Photonics, Multidisciplinary Digital Publishing Institute, 2020, p. 112, vol. 7, no. 4.
[28] X. Jin, S. Zhang, J. Runt, Observation of a fast dielectric relaxation in semi-crystalline poly (ethylene oxide), Polymer 43 (23) (2002) 6247–6254.
[29] A.R. Polu, H.-W. Rhee, The effects of LiTDI salt and POSS-PEG (n= 4) hybrid nanoparticles on crystallinity and ionic conductivity of PEO based solid polymer electrolytes, Sci. Adv. Mater. 8 (5) (2016) 931–940.
[30] A. Azli, N. Manan, M. Kadir, Conductivity and dielectric studies of lithium trifluoromethanesulfonate doped polyethylene oxide-graphene oxide blend based electrolytes, Adv. Mater. Sci. Eng. (2015).
[31] A.A. Ahmad, Q.M. Al-Bataineh, A.A. Bani-Salameh, A.M. Alsaad, A. Telfah, Physicochemical properties of sodium bis (2-methyllactato) borate films doped with iodine for photonic applications, J. Electron. Mater. 51 (11) (2022) 6540–6546.
[32] Q.M. Al-Bataineh, A. Alsaad, A. Ahmad, A. Al-Sawalmih, Structural, electronic and optical characterization of ZnO thin film-seeded platforms for ZnO nanostructures: sol–gel method versus ab initio calculations, J. Electron. Mater. 48 (8) (2019) 5028–5038.
[33] A. Alsaad, Q.M. Al-Bataineh, I. Qattan, A.A. Ahmad, A. Ababneh, Z. Albataineh, I. A. Aljarrah, A. Telfah, Measurement and ab initio investigation of structural, electronic, optical, and mechanical properties of sputtered aluminum nitride thin films, Frontiers in Physics 8 (2020) 115.
[34] S. Noor, A. Ahmad, I. Talib, M.Y. Rahman, Morphology, chemical interaction, and conductivity of a PEO-ENR50 based on solid polymer electrolyte, Ionics 16 (2) (2010) 161–170.
[35] J.-H. Ma, C. Guo, Y.-L. Tang, H.-Z. Liu, 1H NMR spectroscopic investigations on the micellization and gelation of PEO− PPO− PEO block copolymers in aqueous solutions, Langmuir 23 (19) (2007) 9596–9605.
[36] N. El-Ghamaz, H. Ghaly, Effect of chemical and physical doping with iodine on the optical and dielectric properties of poly (vinyl chloride), Chem. Phys. Lett. 648 (2016) 66–74.
[37] I. Fleming, Molecular Orbitals and Organic Chemical Reactions, John Wiley & Sons, 2011.
[38] M. Basappa, L. Yesappa, M. Niranjana, S. Ashokkumar, M. Vandana, H. Vijeth, H. Devendrappa, Structural and optical band gap of PEO/PVP polymer blend, in: AIP Conference Proceedings, AIP Publishing LLC, 2018, p. 140045, vol. 1953, no. 1.
[39] R. Vaz, K.O. Vieira, C.E. Machado, J.L. Ferrari, M.A. Schiavon, Preparation of carbon dots and their optical characterization: an experiment of nanoscience for undergraduate course, Quím. Nova 38 (10) (2015) 1366–1373.
[40] W. Gabes, D. Stufkens, Electronic absorption spectra of symmetrical and asymmetrical trihalide ions, Spectrochim. Acta Mol. Spectros 30 (9) (1974) 1835–1841.
[41] M. Mizuno, J. Tanaka, I. Harada, Electronic spectra and structures of polyiodide chain complexes, J. Phys. Chem. 85 (13) (1981) 1789–1794.
[42] J. Gutierrez, A. Tercjak, I. Garcia, L. Peponi, I. Mondragon, Hybrid titanium dioxide/PS-b-PEO block copolymer nanocomposites based on sol–gel synthesis, Nanotechnology 19 (15) (2008) 155607.
[43] M. Wang, T. Takahama, K. Tashiro, Crystalline iodine complexes of amorphous poly (vinyl acetate) as studied by X-ray diffraction, vibrational spectroscopy, and computer simulation, Macromolecules 53 (11) (2020) 4395–4406.
[44] M. Seto, Y. Maeda, T. Matsuyama, H. Yamaoka, H. Sakai, Mössbauer spectroscopic study of fullerene C60 doped with iodine, Nucl. Instrum. Methods Phys. Res. Sect. B Beam Interact. Mater. Atoms 76 (1–4) (1993) 348–349.
[45] A.A. Ahmad, M.H. Khazaleh, A.M. Alsaad, Q.M. Al-Bataineh, A.D. Telfah, Characterization of As-prepared PVA-PEO/ZnO-Al2O3-NPs hybrid nanocomposite thin films, Polym. Bull. (2021) 1–25.
[46] A. Alsaad, C.M. Marin, N. Alaqtash, H.-W. Chao, T.-H. Chang, C.L. Cheung, A. Ahmad, I. Qattan, R.F. Sabirianov, Crystallographic, vibrational modes and optical properties data of α-DIPAB crystal, Data Brief 16 (2018) 667–684.
[47] M. Oubaha, S. Elmaghrum, R. Copperwhite, B. Corcoran, C. McDonagh, A. Gorin, Optical properties of high refractive index thin films processed at low-temperature, Opt. Mater. 34 (8) (2012) 1366–1370.
[48] E. Davis, N. Mott, Conduction in non-crystalline systems V. Conductivity, optical absorption and photoconductivity in amorphous semiconductors, Phil. Mag. 22 (179) (1970) 903–922.
[49] N.F. Mott, E.A. Davis, Electronic Processes in Non-crystalline Materials, Oxford university press, 2012.
[50] S. Pullen, L.A. Walker, R.J. Sension, Femtosecond studies of the iodine–mesitylene charge-transfer complex, J. Chem. Phys. 103 (18) (1995) 7877–7886.
[51] H. Chamroukhi, Z.B. Hamed, A. Telfah, M. Bassou, A. Zeinert, R. Hergenröder, H. Bouchriha, Optical and structural properties enhancement of hybrid nanocomposites thin films based on polyaniline doped with Zinc Oxide embedded in bimodal mesoporous silica (ZnO@ SiOX) nanoparticles, Opt. Mater. 84 (2018) 703–713.
[52] S. Hemalatha, B. Chandani, D. Balasubramanian, Complexation of molecular iodine by linear poly (ethylene glycol), Spectrosc. Lett. 12 (7–8) (1979) 535–541.
[53] A. Arya, A.L. Sharma, Effect of salt concentration on dielectric properties of li-ion conducting blend polymer electrolytes, J. Mater. Sci. Mater. Electron. 29 (20) (2018) 17903–17920.
[54] A. Arya, A. Sharma, Dielectric relaxations and transport properties parameter analysis of novel blended solid polymer electrolyte for sodium-ion rechargeable batteries, J. Mater. Sci. 54 (9) (2019) 7131–7155.
[55] N. Chilaka, S. Ghosh, Dielectric studies of poly (ethylene glycol)-polyurethane/poly (methylmethacrylate)/montmorillonite composite, Electrochim. Acta 134 (2014) 232–241.
[56] A. Sharma, A.K. Thakur, AC conductivity and relaxation behavior in ion conducting polymer nanocomposite, Ionics (2011) 135–143.
[57] K. Yang, X. Huang, Y. Huang, L. Xie, P. Jiang, Fluoro-polymer@ BaTiO3 hybrid nanoparticles prepared via RAFT polymerization: toward ferroelectric polymer nanocomposites with high dielectric constant and low dielectric loss for energy storage application, Chem. Mater. 25 (11) (2013) 2327–2338.
[58] D.E. Martínez-Tong, L.A. Miccio, A. Alegria, Ionic transport in the amorphous phase of semicrystalline polyethylene oxide thin films, Soft Matter 13 (33) (2017) 5597–5603.
[59] B. Jiang, H. Peng, W. Wu, Y. Jia, Y. Zhang, Numerical simulation and experimental investigation of the viscoelastic heating mechanism in ultrasonic plasticizing of amorphous polymers for micro injection molding, Polymers 8 (5) (2016) 199.
[60] K. Balani, V. Verma, A. Agarwal, R. Narayan, Physical, Thermal, and Mechanical Properties of Polymers, John Wiley & Sons, Inc, Hoboken, NJ, United States, 2014.
[61] B.K. Money, K. Hariharan, J. Swenson, A dielectric relaxation study of nanocomposite polymer electrolytes, Solid State Ionics 225 (2012) 346–349.
[62] J. Ji, B. Li, W.-H. Zhong, Effects of a block copolymer as multifunctional fillers on ionic conductivity, mechanical properties, and dimensional stability of solid polymer electrolytes, J. Phys. Chem. B 114 (43) (2010) 13637–13643.
[63] B.K. Money, K. Hariharan, J. Swenson, Relation between structural and conductivity relaxation in PEO and PEO based electrolytes, Solid State Ionics 262 (2014) 785–789.
[64] A. Kachroudi, A. Kahouli, J. Legrand, F. Jomni, Dielectric and conduction mechanisms of parylene N at high temperature: phase-transition effect, J. Phys. Chem. 119 (24) (2015) 6428–6435.
[65] D.K. Pradhan, R. Choudhary, B. Samantaray, Studies of structural, thermal and electrical behavior of polymer nanocomposite electrolytes, Express Polym. Lett. 2 (9) (2008) 630–638.